# Resonance Raman Evidence for Cleavage of the Fe–$N_\epsilon$(His-F8) Bond in the $\alpha$ Subunit of the T-Structure Nitrosylhemoglobin†

Kiyoshi Nagai, Curtis Welborn, David Dolphin, and Teizo Kitagawa*

ABSTRACT: Resonance Raman spectra are observed for hybrid nitrosylhemoglobins (NO-Hb) reconstituted from normal and meso-deuterated hemes and also for penta- and hexacoordinated NO–heme complexes. Upon meso deuteration of both hemes of the $\alpha$ and $\beta$ subunits [$\alpha(D)_2^{NO}\beta(D)_2^{NO}$], the Raman lines of stripped NO-Hb at 1636 (dp), 1584 (ap), and 1502 (p) $cm^{-1}$ are shifted by −10, −20, and −7 $cm^{-1}$, respectively, and those at 1306 (ap) and 1228 (dp) $cm^{-1}$ disappear. The spectral changes caused by meso deuteration are in good agreement with those observed previously for (octaethylporphyrinato)nickel(II), for which the vibrational assignments of resonance Raman lines have been established. Accordingly, the 1636-, 1584-, 1502-, 1306-, and 1228-$cm^{-1}$ lines of NO-Hb are assigned to $\nu_{10}$, $\nu_{19}$, $\nu_3$, $\nu_{21}$, and $\nu_{13}$, respectively. Upon conversion from the R to the T structure, both $\nu_{19}$ and $\nu_3$ are shifted to higher frequencies by 4 $cm^{-1}$ and $\nu_{10}$ is split into two lines at 1645 and 1637 $cm^{-1}$. The 1645-$cm^{-1}$ line remains unshifted after meso deuteration of the $\beta$ heme [$\alpha(H)_2^{NO}\beta(D)_2^{NO}$], and, conversely, the 1637-$cm^{-1}$ line remains unshifted after meso deuteration of the $\alpha$ heme [$\alpha(D)_2^{NO}\beta(H)_2^{NO}$]. On the basis of the Raman spectra of the model NO–heme complexes, the 1645- and 1637-$cm^{-1}$ lines are assigned to the penta- and hexacoordinated NO–heme complexes. Consequently, we conclude that the Fe–$N_\epsilon$(His-$F_8$) of the $\alpha$ subunit within NO-Hb is disrupted in the T structure, while the NO–heme of the $\beta$ subunit adopts the hexacoordinated structures, in good agreement with our previous electron paramagnetic resonance work. The Raman spectra of the isolated $\alpha^{NO}$ and $\beta^{NO}$ chains are appreciably different. The Raman lines of the isolated $\alpha^{NO}$ chain at 1606 (p), 1587 (ap), and 1504 (p) $cm^{-1}$ are shifted by −6, +5, and +4 $cm^{-1}$ when it is incorporated into the T-structure tetramer. In contrast, all the Raman lines of the isolated $\beta^{NO}$ chain are not shifted in the T-structure tetramer.

Hemoproteins with a common prosthetic group at the active center can conduct various biochemical reactions. Such a variety of biological functions is attributed, in part, to different structural and electronic properties of the heme produced when it is incorporated into different proteins. Resonance Raman scattering from hemoproteins excited within the visible absorption bands mostly arises from vibrations of the porphyrin ring (Spiro, 1975; Felton & Yu, 1978; Kitagawa et al., 1978a), and the frequencies of Raman lines have been interpreted in terms of the stereochemistry or electronic properties of the heme (Spaulding et al., 1975; Spiro et al., 1979; Kitagawa et al., 1976; Teraoka & Kitagawa, 1980). Based on the empirical relationship thus obtained, resonance Raman spectroscopy has provided unique and important information on the heme moiety of the proteins.

Hemoglobin (Hb)[1] can exist in two alternative quaternary structures: the T structure with low oxygen affinity and the R structure with high oxygen affinity (Perutz, 1970; Monod et al., 1965). Recently, we assigned the Raman line of deoxy-Hb at 216 $cm^{-1}$ to the Fe–$N_\epsilon$(His-F8) stretching mode (Kitagawa et al., 1979; Nagai et al., 1980; Hori & Kitagawa, 1980). The frequency shift of the Fe–$N_\epsilon$(His-F8) stretching mode observed upon the conversion of quaternary structure has evidenced a stretch of the Fe–$N_\epsilon$(His-F8) bond of deoxy-Hb in the T structure (Nagai et al., 1980; Nagai & Kitagawa, 1980). Small but definite frequency shifts have also been observed in the higher frequency porphyrin modes (Shelnutt et al., 1979).

NO-Hb normally adopts the R structure but it is converted to the T structure by addition of inositol hexaphosphate (IHP). Structural change of the heme in NO-Hb upon the switch of quaternary structure has been monitored with various spectroscopic methods including visible absorption (Perutz et al., 1976; Rein et al., 1972; Salhany et al., 1974, 1975; Cassoly, 1974), infrared (Maxwell & Caughey, 1976), EPR (Szabo & Perutz, 1976; Nagai et al., 1978), and Raman spectra (Szabo & Barron, 1975; Scholler et al., 1979). These studies demonstrated that NO-Hb with the R structure lies in the normal hexacoordinated structure, but NO-Hb with the T structure is an equimolar mixture of the penta- and hexacoordinated NO–heme complexes. Perutz et al. (1976) and Nagai et al. (1978) suggested that the $\alpha$ subunit is responsible for the unusual pentacoordinated NO–heme complex. In the present study we have confirmed this suggestion, with Raman spectroscopy, through labeling the $\alpha$ or the $\beta$ subunit with the isotope-substituted heme.

## Materials and Methods

*Preparation of Meso-Deuterated Protoporphyrin IX.* Protoporphyrin IX *meso-*$d_4$ free acid was prepared directly via magnesium protoporphyrin which rapidly exchanges its meso protons in solution under conditions where the vinyl substituents are unaffected. The modified procedure involved heating free acid protoporphyrin IX (200 mg) under argon at 125 °C for 4 h in 10 mL of the magnesium reagent described by Kenner et al. (1978). After the addition of methanol-$d_1$ (2.0 mL, 99.5% *d*), the mixture was heated at 100 °C for 1.5 h. The solution was evaporated to dryness in vacuo, residue was dissolved in tetrahydrofuran (50 mL), and

† From the Second Department of Physiology, Nara Medical University, Kashihara, Nara, 634, Japan (K.N.), the Department of Chemistry, The University of British Columbia, Vancouver, British Columbia V6T 1W5, Canada (C.W. and D.D.), and the Department of Molecular Physiological Chemistry, Medical School, Osaka University, Kita-ku, Osaka, 530, Japan (T.K.). *Received April 9, 1980.* Supported by a grant from the National Institutes of Health (AM 17989) to D.D. and C.W.

[1] Abbreviations used: Hb, hemoglobin; Mb, myoglobin; PP, protoporphyrin IX; OEP, octaethylporphyrin, PPDME, protoporphyrin dimethyl ester; TPP, *meso*-tetraphenylporphyrin; IHP, inositol hexaphosphate; $NaDodSO_4$, sodium dodecyl sulfate; 2-MeIm, 2-methylimidazole; *N*-MeIm, *N*-methylimidazole; 4-MePip, 4-methylpiperidine; EPR, electron paramagnetic resonance; p, polarized; dp, depolarized; ap, anomalously polarized; $\alpha$(D) and $\beta$(D), $\alpha$ and $\beta$ subunits reconstituted with the meso-deuterated heme; $\alpha$(H) and $\beta$(H), $\alpha$ and $\beta$ subunits with normal heme; DMF, dimethylformamide; CM, carboxymethyl.

0006-2960/80/0419-4755$01.00/0 

trifluoroacetic acid-$d_1$ (5 mL) was added to demetalate the porphyrin.

On completion of demetalation (disappearance of the 548- and 587-nm visible bands), the solution was poured into ice water (200 mL), and the precipitated porphyrin was collected by filtration, washed with cold water, and dried in vacuo. Iron was inserted by heating the recovered, dried porphyrin (200 mg) in DMF (15 mL) under argon at 160 °C for 15 min. The hemin was recovered by pouring the DMF solution into ice-cold 1% HCl (100 mL), filtering off the ferric protoporphyrin IX chloride free acid, washing with cold water, and drying in vacuo immediately.

Neither the free acid porphyrin nor the free acid hemin can be efficiently purified by chromatography; thus, the purity of the product is dependent on the purity of the starting protoporphyrin and on the protection of the reactive vinyl substituents from light, oxygen, and acids. The deuterium content was determined by mass spectral analysis of the porphyrin dimethyl ester, prepared by esterification in 5% methanolic $H_2SO_4$. Preparations using this procedure ranged from 88 to 93% $d_4$. Mass spectral analysis indicated that no deuterium loss occurred during iron insertion or esterification.

*Preparation of Hemoglobin.* Human adult hemoglobin was prepared as described by Kilmartin & Rossi-Bernardi (1970) and gel filtered against 0.05 M sodium phosphate buffer, pH 7.2 (1.42 g/L $NaH_2PO_4 \cdot 2H_2O$ and 3.02 g/L $Na_2HPO_4$). The Hb solution was applied to a column of Bio-Rex 70 (Bio-Rad, Inc.) equilibrated with the same buffer. After elution of glycosylated minor hemoglobins (Hb $A_1$), major Hb A was eluted with 0.1 M sodium phosphate buffer, pH 7.2. The isolated $\alpha$ and $\beta$ chains were prepared in the CO forms as described by Kilmartin et al. (1975).

*Preparation of $\alpha(H)_2\beta(D)_2$ and $\alpha(D)_2\beta(H)_2$.* Preparation of globin solution and reconstitution of Hb were carried out as described by Yonetani & Asakura (1968) with slight modification. Met-Hb was prepared by addition of 1.2 equiv of $K_3Fe(CN)_6$ solution to oxy-Hb at 37 °C and was dialyzed against cold deionized water overnight. The met-Hb solution was adjusted to pH 2.5 with 0.1 N HCl and transferred into a separatory funnel together with 2 volumes of well-chilled butanone. The mixture was shaken and the lower phase was collected. This procedure was repeated if the removal of the heme was incomplete. The globin solution thus obtained was dialyzed against several changes of cold distilled water and 0.002 M $NaHCO_3$ and finally against 0.01 M Tris-HCl buffer, pH 8.6. After the precipitate was spun down, the concentration of the globin solution was determined by spectrophotometric titration with diluted hemin solution at 405 nm. A 15-mg sample of either protohemin (Sigma Chemical Co., bovine type II) or meso-deuterated iron protoporphyrin IX was dissolved in 0.5 mL of 0.1 N NaOH solution and diluted with 20 mL of distilled water. The globin solution was mixed with hemin solution in a molar ratio of 1:1.05. Hereafter, we represent the reconstituted Hb with normal hemin as $\alpha(H)_2\beta(H)_2$ and that with meso-deuterated hemin as $\alpha(D)_2\beta(D)_2$ and hybrid Hb's as $\alpha(H)_2\beta(D)_2$ or $\alpha(D)_2\beta(H)_2$. The reconstituted met-Hb was reduced with a minimal amount of sodium dithionite solution under an atmosphere of CO and dialyzed against several changes of 0.01 M Tris-HCl buffer, pH 8.0, saturated with CO and finally against 0.01 M sodium phosphate buffer, pH 6.0 (1.458 g/L $NaH_2PO_4 \cdot 2H_2O$ and 0.093 g/L $Na_2HPO_4$). The reconstituted CO-Hb was applied to a 2 × 10 cm column of CM-52 cellulose (Whatman) and eluted with a linear gradient in 500 mL of 0.01 M sodium phosphate buffer, pH 6.0, and 500 mL of 0.07 M sodium phosphate buffer, pH 6.9 (3.164 g/L $NaH_2PO_4 \cdot 2H_2O$ and 3.528 g/L $Na_2HPO_4$). The main peak was collected and concentrated by ultrafiltration using a UK-10 membrane (Toyo Roshi, Inc.).

The isolated $\alpha$(D) and $\beta$(D) chains were prepared by following the method of Kilmartin et al. (1975) and were recombined with $\alpha$(H) and $\beta$(H) chains in the presence of dithiothreitol (5 mg/mL) under an atmosphere of CO with the condition that a 5% excess of $\beta$ chain was present compared with the amount of $\alpha$ chain. The hybrid Hb solutions were gel filtered against 0.01 M sodium phosphate buffer, pH 6.9, and the excess $\beta$ chain was removed by passage through a column of DE-52 cellulose (Whatman) equilibrated with the same buffer. All Hb solutions were gel filtered against 1 mM $Na_2HPO_4$ and deionized by passage through a Dintzis column (Nozaki & Tanford, 1967). The oxygen equilibrium curves of these hybrids were measured with Dr. Imai's apparatus (Imai et al., 1970) and were found to be identical with native Hb in the range between 10 and 90% oxygen saturation.

*Preparation of Nitrosylhemoglobin.* Hb was diluted with an appropriate buffer and equilibrated with CO gas to ensure that all hemes were saturated with CO. Free oxygen and CO were removed by repeated evacuation and flushing with $N_2$ gas in a cylindrical cell fitted with a rubber teat. NO gas vigorously shaken with 0.1 N NaOH solution was injected into the cell through the rubber teat with an air-tight syringe. By this procedure, even high-affinity Hb's such as the isolated $\alpha$ and $\beta$ chains can be converted to the nitrosyl form without using sodium dithionite. The isolated $\alpha^{NO}$ and $\beta^{NO}$ chains thus obtained were stable for several days even at room temperature.

*Preparation of Penta- and Hexacoordinated NO–Heme Complexes.* Hemin (Sigma, bovine type I) was dissolved in diluted alkaline solution or in a 2% sodium dodecyl sulfate ($NaDodSO_4$) aqueous solution at alkaline pH. Both solutions were freed from oxygen in the Raman cell and equilibrated with NO gas which had been shaken with 0.1 N NaOH solution. The hemin solutions were spontaneously reduced to produce pentacoordinated NO–heme complexes.

Protohemin dimethyl ester (PPDME) was prepared according to the method described by Fuhrhop & Smith (1975). Pentacoordinated iron(II) protoporphyrin dimethyl ester–NO [(PPDME)$Fe^{II}$(NO)] was prepared in $CH_2Cl_2$ solution by reductive nitrosylation in the presence of 5% methanol. The hexacoordinated (PPDME)$Fe^{II}$(NO)(*N*-MeIm) was prepared by further addition of 10 volumes of deaerated *N*-methylimidazole (*N*-MeIm).

*Measurement of Raman Spectra.* Raman scattering was excited with the 488.0-nm line of an argon ion laser (Spectra Physics, Model 164) and was recorded on a JEOL-400D Raman spectrometer. The incident radiation was introduced from the bottom of the cell, and the scattered radiation along 90° from the incident radiation was collected. The Raman spectrometer was calibrated with indene (Hendra & Loader, 1961). Instrumental settings were common to all measurements unless otherwise stated (Figure 1) and are described in the caption of Figure 2.

## Results

The polarized resonance Raman spectra of stripped $\alpha(H)_2{}^{NO}\beta(H)_2{}^{NO}$ and $\alpha(D)_2{}^{NO}\beta(D)_2{}^{NO}$ excited at 488.0 nm are shown in Figure 1, where the solid line and broken line indicate the parallel and perpendicular polarization components, respectively. Upon meso deuteration, the Raman lines of $\alpha(H)_2{}^{NO}\beta(H)_2{}^{NO}$ at 1636 (dp), 1584 (ap), and 1502 (p) $cm^{-1}$ (p, dp, and ap denote the polarized, depolarized, and anom-

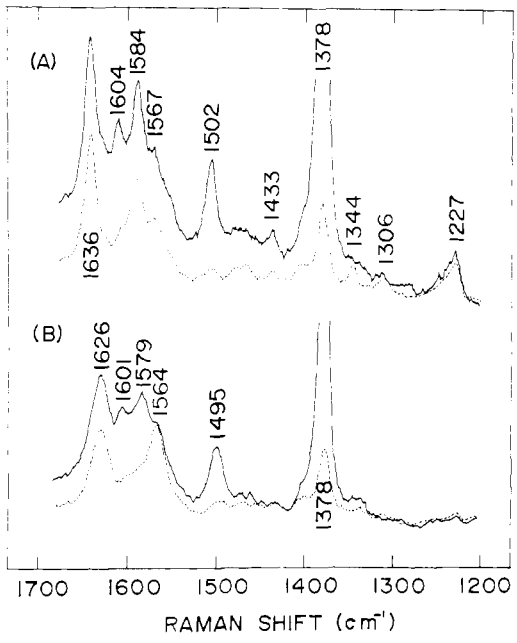


FIGURE 1: Polarized resonance Raman spectra of stripped $\alpha$-$(H)_2{}^{NO}\beta(H)_2{}^{NO}$ (A) and $\alpha(D)_2{}^{NO}\beta(D)_2{}^{NO}$ (B). The solid line and broken line indicate the electric vector of the scattered radiation to be parallel and perpendicular to that of the incident radiation, respectively. Laser power, 80 mW; sensitivity, 250 counts/s; time constant, 16 s; scan speed, 10 $cm^{-1}$/min; slit width, 4 $cm^{-1}$.

alously polarized lines, respectively) are shifted to 1626, 1564, and 1495 $cm^{-1}$, respectively, and the lines at 1306 (ap) and 1227 (dp) $cm^{-1}$ disappear from this frequency range, although a weak feature remains at 1226 $cm^{-1}$ in the spectrum of $\alpha$-$(D)_2{}^{NO}\beta(D)_2{}^{NO}$ due to incomplete meso deuteration. The observed meso deuteration shifts are in good agreement with those observed for (octaethylporphyrinato)nickel(II) [(OEP)$Ni^{II}$] ($\Delta\nu_{10} = -10$, $\Delta\nu_{19} = -21$, $\Delta\nu_3 = -7$, $\Delta\nu_{21} = -418$, and $\Delta\nu_{13} = -270$ $cm^{-1}$) (Kitagawa et al., 1978b; Spaulding et al., 1975).

Figure 2 shows the resonance Raman spectra of stripped NO-Hb's derived from $\alpha(H)_2\beta(D)_2$ (A), $\alpha(H)_2\beta(H)_2$ (B), $\alpha(D)_2\beta(H)_2$ (C), and $\alpha(D)_2\beta(D)_2$ (D). If the Raman spectra of the $\alpha$ and $\beta$ subunits were exactly the same, $\alpha(D)_2{}^{NO}\beta$-$(H)_2{}^{NO}$ and $\alpha(H)_2{}^{NO}\beta(D)_2{}^{NO}$ should exhibit the same Raman spectrum, which would be an arithmetic mean of the spectra shown in parts B and D of Figure 1. When two Raman lines with similar intensities but with slightly different frequencies are unresolved, one peak is observed at their midpoint frequencies; thus spectra A and C are approximately the mean of spectra B and D. However, the 1634-$cm^{-1}$ line of $\alpha$-$(H)_2{}^{NO}\beta(D)_2{}^{NO}$ (A) displays a pronounced shoulder which is absent in the spectrum of $\alpha(D)_2{}^{NO}\beta(H)_2{}^{NO}$ (C). The shoulder arises from the meso-deuterated heme. This implies slight differences in frequency and intensity between the $\alpha^{NO}$ and $\beta^{NO}$ subunits.

Figure 3 shows the resonance Raman spectra of the isolated $\alpha(H)^{NO}$ and $\beta(H)^{NO}$ chains. Although Scholler et al. (1979) failed to observe the Raman spectrum of the $\alpha^{NO}$ chain due to instability, our preparations of $\alpha^{NO}$ and $\beta^{NO}$ chains were perfectly stable at room temperature even under laser illumination. The Raman lines of the $\beta^{NO}$ chain at 1636, 1604, 1584, 1567, and 1501 $cm^{-1}$ are shifted slightly to higher frequencies in the $\alpha^{NO}$ chain. Moreover, the 1636-$cm^{-1}$ line of the $\beta^{NO}$ chain is more intense than the 1638-$cm^{-1}$ line of the $\alpha^{NO}$ chain. In analogy with this, the corresponding Raman line of the meso-deuterated heme is expected to be at lower frequency with higher intensity in the $\beta$(D) chain than in the

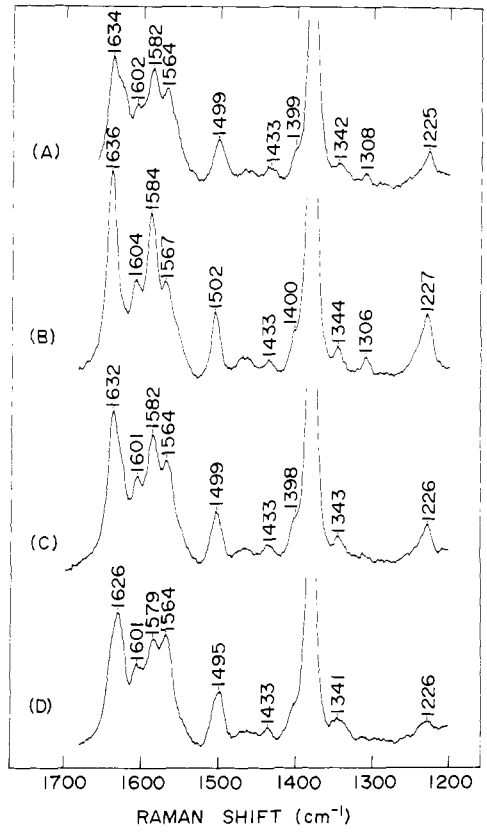


FIGURE 2: Resonance Raman spectra of stripped NO-Hb: (A) $\alpha(H)_2{}^{NO}\beta(D)_2{}^{NO}$; (B) $\alpha(H)_2{}^{NO}\beta(H)_2{}^{NO}$; (C) $\alpha(D)_2{}^{NO}\beta(H)_2{}^{NO}$; (D) $\alpha(D)_2{}^{NO}\beta(D)_2{}^{NO}$. Experimental conditions: buffer, 0.05 M Bis-Tris, 0.05 M Tris, and 0.1 M $Cl^{-1}$, pH 6.5; scan speed, 10 $cm^{-1}$/min; slit width, 4 $cm^{-1}$; time constant, 8 s; laser power, 60 mW; sensitivity, 500 counts/s.

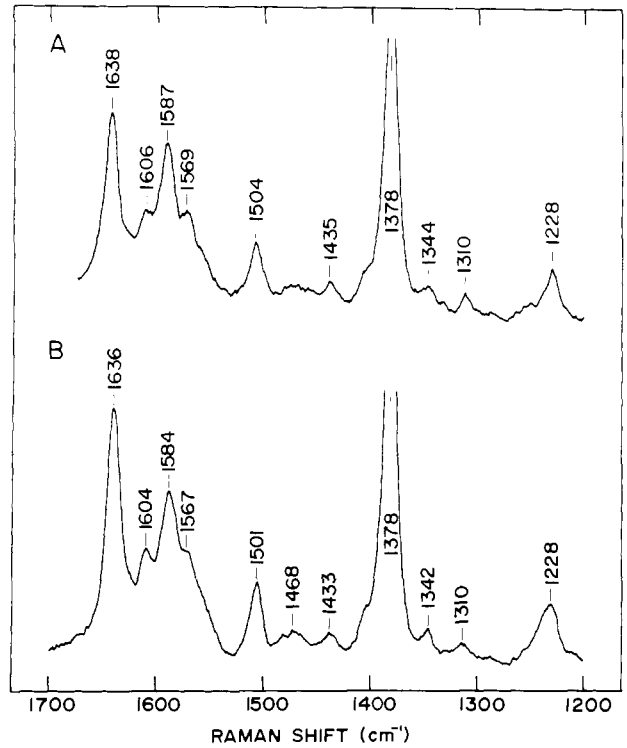


FIGURE 3: Resonance Raman spectra of the isolated $\alpha^{NO}$ (A) and $\beta^{NO}$ (B) chains. Experimental conditions are as in Figure 2.

$\alpha$(D) chain. This may cause the appearance of the Raman line of the deuterated heme as a shoulder for $\alpha(H)_2{}^{NO}\beta(D)_2{}^{NO}$ but not for $\alpha(D)_2{}^{NO}\beta(H)_2{}^{NO}$.

Table I: Frequencies of Raman Lines of NO-Hb and NO-Heme Complexes ($cm^{-1}$)[a]

| | assignment[b] | $\rho_1$[c] | $\Delta\nu$[d] | stripped NO-Hb | $\alpha^{NO}$ chain | $\beta^{NO}$ chain | NO-Hb with IHP: $\alpha^{NO}$ subunit | NO-Hb with IHP: $\beta^{NO}$ subunit | pentaco-ordinated NO-heme[e] | hexaco-ordinated NO-heme[f] |
|---|---|---|---|---|---|---|---|---|---|---|
| 1 | $\nu_{10}$ | dp | −10 | 1636 | 1638 | 1636 | 1645 | 1635 | 1647 | 1637 |
| 2 | $\nu_2$ | p | −3 | 1604 | 1606 | 1604 | 1600 | 1602 | sh[j] | sh |
| 3[i] | $\nu_{19}$ | ap | −20 | 1584 | 1587 | 1584 | 1592 | 1584 | 1588 | 1585 |
| 4 | $\nu_{11}$ | dp | −3 | 1567 | 1569 | 1567 | 1568 | 1567 | 1565 | |
| 5 | $\nu_3$ | p | −7 | 1502 | 1504 | 1501 | 1508 | 1501 | 1508 | |
| 6[g] | | dp | 0 | 1433 | 1435 | 1433 | 1433 | 1434 | 1435 | |
| 7[h] | $\nu_{20}$ | ap | 0 | 1400 | 1400 | 1400 | 1402 | 1398 | 1403 | |
| 8 | $\nu_4$ | p | 0 | 1378 | 1378 | 1378 | 1378 | 1378 | 1376 | |
| 9[g] | | ap | 0 | 1344 | 1344 | 1342 | 1346 | 1345 | 1342 | |
| 10[g] | $\nu_{21}$ | ap | | 1306 | 1310 | 1310 | 1306 | 1308 | 1300 | |
| 11 | $\nu_{13}$ | dp | | 1227 | 1228 | 1228 | 1225 | 1227 | 1227 | |

[a] Accuracy ±1 $cm^{-1}$. [b] Mode numbers are taken from Abe et al. (1978). [c] Depolarization ratio: p, polarized; dp, depolarized; ap, anomalously polarized. [d] Frequency shift observed for stripped NO-Hb upon meso deuteration. [e] (PP)$Fe^{II}$(NO) in aqueous $NaDodSO_4$ solution. [f] (PPDME)$Fe^{II}$(NO)(*N*-MeIm) in *N*-MeIm. [g] Accuracy ±2 $cm^{-1}$. [h] Accuracy ±3 $cm^{-1}$. [i] This line is overlapped with the polarized line which shifts to 1579 $cm^{-1}$ upon meso deuteration. [j] sh, shoulder.

Figure 4 shows the resonance Raman spectra of the T-structure NO-Hb's derived from $\alpha(H)_2\beta(D)_2$ (A), $\alpha(H)_2\beta(H)_2$ (B), $\alpha(D)_2\beta(H)_2$ (C), and $\alpha(D)_2\beta(D)_2$ (D). In comparison of Figure 4B with Figure 2B, it is apparent that the 1636-$cm^{-1}$ line of the R-structure NO-Hb is split into the lines at 1645 and 1637 $cm^{-1}$. This splitting was first pointed out by Szabo & Barron (1975) and is confirmed in this experiment. In addition, the 1604-, 1584-, and 1502-$cm^{-1}$ lines of the R-structure NO-Hb (Figure 2B) are shifted to 1602, 1588, and 1506 $cm^{-1}$, respectively, in the T-structure NO-Hb (Figure 4B).

When the heme of the $\beta$ subunit is replaced by the meso-deuterated heme, the 1645-$cm^{-1}$ line remains unshifted but the 1637-$cm^{-1}$ line is shifted to 1624 $cm^{-1}$ as shown in the spectrum of $\alpha(H)_2{}^{NO}\beta(D)_2{}^{NO}$ (A). When the heme of the $\alpha$ subunit is replaced by the meso-deuterated heme, the 1637-$cm^{-1}$ line remains unshifted. Therefore, it is proved that the 1645- and 1637-$cm^{-1}$ lines of the T-structure $\alpha(H)_2{}^{NO}\beta(H)_2{}^{NO}$ arise from the $\alpha$ and $\beta$ subunits, respectively.

The 1506-$cm^{-1}$ line of $\alpha(H)_2{}^{NO}\beta(H)_2{}^{NO}$ is split into two lines at 1508 and 1494 $cm^{-1}$ in $\alpha(H)_2{}^{NO}\beta(D)_2{}^{NO}$ but is apparently shifted to 1503 $cm^{-1}$ in $\alpha(D)_2{}^{NO}\beta(H)_2{}^{NO}$ (Figure 4). This mode is expected to show a low-frequency shift by ~7 $cm^{-1}$ upon meso deuteration as shown in Figure 1. Figure 4A indicates that the corresponding Raman lines of the $\alpha(H)^{NO}$ and $\beta(D)^{NO}$ subunits are at 1508 and 1494 $cm^{-1}$, respectively. Then for $\alpha(H)_2{}^{NO}\beta(H)_2{}^{NO}$, two Raman lines are expected at 1508 and 1501 $cm^{-1}$, but they are not actually resolved in Figure 4B and give one peak at the average frequency weighted by individual intensities. On the other hand, for $\alpha(D)_2{}^{NO}\beta(H)_2{}^{NO}$, the corresponding lines are expected at 1501 $cm^{-1}$ for the $\alpha(D)^{NO}$ subunit and at 1501 $cm^{-1}$ for the $\beta(H)^{NO}$ subunit. Accordingly one symmetric peak at 1503 $cm^{-1}$ for $\alpha(D)_2{}^{NO}\beta(H)_2{}^{NO}$ seems reasonable.

When both hemes are deuterated, the Raman lines are expected at 1501 and 1494 $cm^{-1}$ but are again unresolved and observed at the average frequency weighted by the intensity. In similar comparative considerations, the frequencies of Raman lines of the $\alpha$ and $\beta$ subunits are determined as listed in Table I. Note that the frequencies of the $\alpha$ and $\beta$ subunits in the T-structure tetramer differ from those of the isolated $\alpha$ and $\beta$ subunits.

Figure 5 shows the resonance Raman spectra of penta- and hexacoordinated model NO–heme complexes. The two spectra of the pentacoordinated complexes, namely, (protoporphyrinato)Fe(II)–NO [(PP)$Fe^{II}$(NO)] in the aqueous $NaDodSO_4$ solution (A) and (PPDME)$Fe^{II}$(NO) in $CH_2Cl_2$

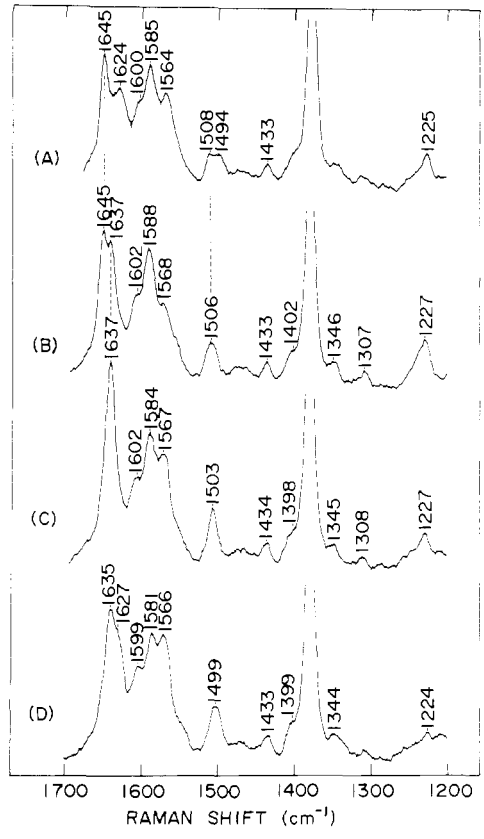


FIGURE 4: Resonance Raman spectra of NO-Hb in the presence of 2 mM IHP: (A) $\alpha(H)_2{}^{NO}\beta(D)_2{}^{NO}$; (B) $\alpha(H)_2{}^{NO}\beta(H)_2{}^{NO}$; (C) $\alpha(D)_2{}^{NO}\beta(H)_2{}^{NO}$; (D) $\alpha(D)_2{}^{NO}\beta(D)_2{}^{NO}$. Experimental conditions are as in Figure 2.

(B), are alike, although the latter is partly masked by strong Raman lines of the solvent. Since the hexacoordinated (PPDME)$Fe^{II}$(NO)(*N*-MeIm) is formed only in the presence of a large excess of *N*-MeIm, a part of the Raman spectrum is masked by the Raman lines of *N*-MeIm. However, it is apparent that the pentacoordinated complexes give the highest frequency mode at 1646–1647 $cm^{-1}$, while the hexacoordinated one gives it at 1637 $cm^{-1}$. These frequencies closely agree with 1645 $cm^{-1}$ ($\alpha$ subunit) and 1637 $cm^{-1}$ ($\beta$ subunit) of the T-structure NO-Hb.

## Discussion

*Distinction of $\alpha$ and $\beta$ Subunits.* The Raman spectrum of NO-Hb undergoes changes upon the R → T transition as first pointed out by Szabo & Barron (1975), although they did not

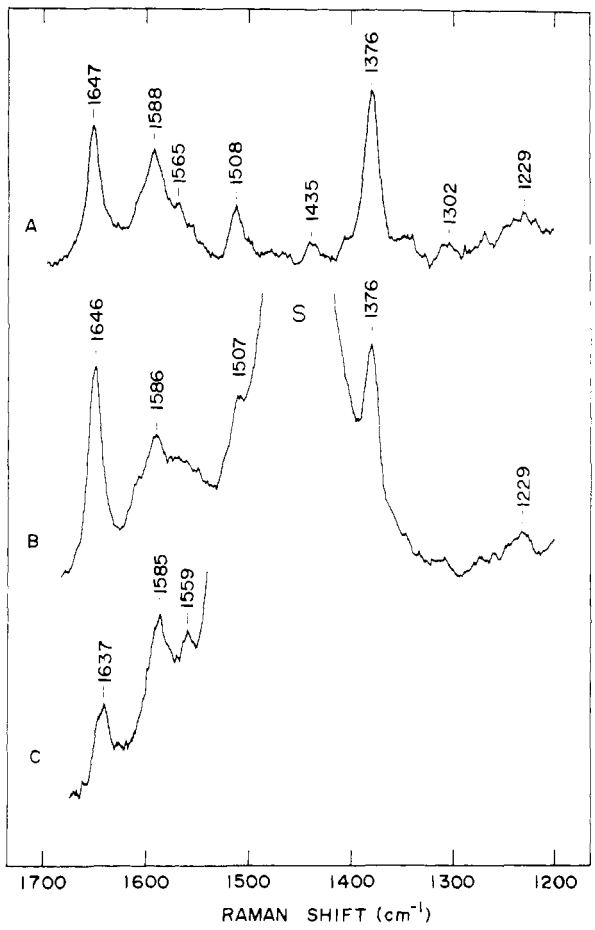


FIGURE 5: Resonance Raman spectra of NO–heme complexes: (A) (PP)$Fe^{II}$(NO) in 2% $NaDodSO_4$ aqueous solution; (B) (PPDME)-$Fe^{II}$(NO) in $CH_2Cl_2$ with 5% methanol; (C) (PPDME)$Fe^{II}$(NO)(*N*-MeIm) in *N*-MeIm with 9% $CH_2Cl_2$. Instrumental conditions are as in Figure 2.

interpret the splitting of the 1636-$cm^{-1}$ line of the R-structure NO-Hb into two lines at 1645 and 1637 $cm^{-1}$ in the T-structure NO-Hb. By using hybrid NO-Hb's such as $\alpha$-$(D)_2{}^{NO}\beta(H)_2{}^{NO}$ and $\alpha(H)_2{}^{NO}\beta(D)_2{}^{NO}$, we have clearly demonstrated that the 1645- and 1637-$cm^{-1}$ lines arise from the $\alpha^{NO}$ and $\beta^{NO}$ subunits, respectively. The present results from the model compounds, together with the work by Scholler et al. (1979), suggest that the 1647- and 1637-$cm^{-1}$ lines are associated with the penta- and hexacoordinated NO–heme complexes, respectively. Consequently, it is concluded that the NO–hemes of the $\alpha$ and $\beta$ subunits assume the penta- and hexacoordinated structures, respectively, in the T-structure tetramer, but both hemes adopt the hexacoordinated structure in the R-structure tetramer. This means that the Fe–$N_\epsilon$-(His-F8) bond in the $\alpha$ subunit is disrupted in the T structure.

This conclusion is consistent with the EPR work by Nagai et al. (1978), who found that the $\alpha^{NO}$ subunit of the T-structure NO-Hb exhibits a strong triplet-hyperfine structure centered at $g = 2.009$, characteristic of the pentacoordinated NO–heme complexes, while the $\beta$ subunit lacks the triplet. Perutz et al. (1976), on the other hand, suggested that the $\alpha$ subunit is predominantly responsible for the changes in the visible and Soret absorption spectra of NO-Hb upon addition of IHP. Maxwell & Caughey (1976) pointed out that the NO-stretching infrared band of the R-structure NO-Hb at 1668 $cm^{-1}$ is split into two bands at 1615 and 1668 $cm^{-1}$ in the T structure, the former of which was assigned to the pentacoordinated NO–heme complex on the basis of studies of model compounds. The present study suggests that the 1615- and 1668-$cm^{-1}$ NO-stretching bands arise from the $\alpha$ and $\beta$ subunits, respectively, of the T-structure NO-Hb.

In accord with the structural change of the $\alpha$ subunit upon conversion to the T structure, the 1606- (p), 1587- (ap), and 1504- (p) $cm^{-1}$ lines of the isolated $\alpha^{NO}$ chain are shifted by −6, +5, and +4 $cm^{-1}$ in the T-structure tetramer (see Table I). In contrast, all the Raman lines of the isolated $\beta^{NO}$ chain are not shifted in the T-structure tetramer.

It is also interesting to note that the Raman spectra of the isolated $\alpha^{NO}$ and $\beta^{NO}$ chains appreciably differ, as shown in Figure 3. Shiga et al. (1969) first pointed out that the isolated $\alpha^{NO}$ and $\beta^{NO}$ chains exhibit dissimilar EPR spectra. The EPR spectrum of the $\beta^{NO}$ chain changes significantly in the temperature range 77–4.2 K, whereas that of the $\alpha^{NO}$ chain remains almost unchanged (Nagai et al., 1978). Furthermore, the EPR spectra of NO-Hb and absorption spectra of its photolyzed form are sensitively altered by amino acid replacements at His-E7 and Val-E11 (Nagai et al., 1979). These results suggest that the surrounding amino acid residues such as Val-E11 and His-E7 (distal histidine) impose restriction to the Fe–NO bonding mode, resulting in the spectral difference between the $\alpha^{NO}$ and $\beta^{NO}$ chains.

Scholler et al. (1979) reported some inconsistency between the EPR and Raman results. According to them, the $\alpha^{NO}$ chain exhibits the triplet hyperfine in the EPR spectrum at low pH but not the Raman line at 1647 $cm^{-1}$. However, our EPR spectrum of the $\alpha^{NO}$ chain reported earlier (Nagai et al., 1978) appeared quite consistent with the Raman results reported here. It is important that the isolated $\alpha^{NO}$ chain exhibits neither the triplet hyperfine nor the Raman line at 1647 $cm^{-1}$, even at low pH, unless it is incorporated into the tetramer and converted to the T structure.

*Interpretation of Raman Spectra.* Several Raman lines of NO-Hb exhibited low-frequency shifts upon meso deuteration of the heme. The observed isotopic frequency shift and polarization properties appeared quite consistent with those observed for (OEP)$Ni^{II}$ for which all the Raman lines have been interpreted on the basis of the isotopic frequency shifts (Kitagawa et al., 1978b) and subsequent normal coordinate calculations (Abe et al., 1978). Therefore, the assignment proposed for (OEP)$Ni^{II}$ seems applicable to NO-Hb.

The Raman lines of the pentacoordinated NO–heme complex at 1645 (dp), 1592 (ap), and 1508 (p) $cm^{-1}$ ($\alpha^{NO}$ subunit in NO-Hb with IHP) are shifted to 1635, 1584, and 1501 $cm^{-1}$ in the hexacoordinated NO–heme complex ($\beta^{NO}$ subunit in NO-Hb with IHP). The former three lines correspond well to the Raman lines of (PP)$Fe^{II}$(NO) at 1647, 1588, and 1508 $cm^{-1}$. The three lines are mainly associated with the $C_\alpha$–$C_m$ stretching modes of the $B_{1g}$ (dp, $\nu_{10}$), $A_{2g}$ (ap, $\nu_{19}$), and $A_{1g}$ (p, $\nu_3$) species, respectively, in the approximation of $D_{4h}$ symmetry (Abe et al., 1978).

The molecular structures of the penta- and hexacoordinated (TPP)$Fe^{II}$(NO)L (L = none, *N*-MeIm, or 4-MePip) were analyzed by Scheidt and co-workers (Scheidt & Frisse, 1975; Scheidt & Piciulo, 1976; Scheidt et al., 1977). According to them, the Fe–$C_t$ distance is longer in the pentacoordinated complex (0.211 Å) than in the hexacoordinated one (0.07 Å). This may imply less delocalization of electrons from iron to porphyrin in the pentacoordinated complex. On the other hand, it was previously pointed out that decreased occupation of electrons in the antibonding $\pi^*$ orbital of the porphyrin ring raises the vibrational frequencies of some porphyrin modes (Spiro & Strekas, 1974; Kitagawa et al., 1976). Accordingly, the higher frequencies of porphyrin modes in the pentacoordinated NO–heme complexes are presumably caused by

the decreased back-donation from the iron $d_\pi$ to porphyrin $\pi^*$ orbitals. In fact, the $C_\alpha$–$C_m$ bond length is 1% longer in the hexacoordinated compound [1.399 Å for (TPP)$Fe^{II}$(NO)(*N*-MeIm) and 1.390 Å for (TPP)$Fe^{II}$(NO)], and therefore its lower stretching frequency in the hexacoordinated complex is consistent with the molecular structure. Since the NO-stretching frequency observed with infrared spectroscopy is lower in the hexacoordinated complex (1625 $cm^{-1}$) than in the pentacoordinated complex (1670 $cm^{-1}$) (Scheidt et al., 1977), $\pi$ back-donation from iron $d_\pi$ to nitrosyl $\pi^*$ would be larger in the hexacoordinated complex. Thus, when imidazole is bound to the trans position of NO in the heme, the $\pi$ back-donation to the nitrosyl $\pi^*$ orbital and the porphyrin $\pi^*$ electron occupation might increase simultaneously.

*Implications to Mechanism of Heme–Heme Interaction.* The oxygen affinity of the $\alpha$ and $\beta$ subunits within Hb are equally lowered upon the R → T transition. Why is the Fe–$N_\epsilon$(His-F8) bond of NO-Hb disrupted in the $\alpha$ subunit but not in the $\beta$ subunit? Recently we compared the Fe–$N_\epsilon$(His-F8) stretching frequencies of the $\alpha$ and $\beta$ subunits within deoxy-Hb. Upon conversion from the R to the T structure, the Fe–$N_\epsilon$(His-F8) stretching frequency changes from 223 to 203 $cm^{-1}$ in the $\alpha^{deoxy}$ subunit and from 224 to 217 $cm^{-1}$ in the $\beta^{deoxy}$ subunit (Nagai & Kitagawa, 1980). Therefore, the Fe–$N_\epsilon$(His-F8) bond length is stretched three times more in the $\alpha$ subunit than the $\beta$ subunit. Thus, the withdrawing force imposed to $N_\epsilon$ of His-F8 by protein in the T structure (Perutz, 1970) must be stronger in the $\alpha$ subunit than in the $\beta$ subunit.

According to the X-ray crystallographic analysis of NO–porphyrin model compounds (Scheidt & Frisse, 1975; Scheidt & Piciulo, 1976), the heme iron is displaced toward NO. The displacement from the mean plane of four pyrrole nitrogens ($N_{pyrr}$) is 0.211 and 0.07 Å for the penta- and hexacoordinated NO–heme model compounds, respectively. The Fe–NO bond length is longer for the hexacoordinated compound than for the pentacoordinated one [1.717 Å for (TPP)$Fe^{II}$(NO) and 1.743 Å for (TPP)$Fe^{II}$(NO)(*N*-MeIm)], but their porphyrin core sizes are alike. This means that repulsive interaction between $N_{pyrr}$ and NO is particularly important.

If $N_\epsilon$ of His-F8 withdrew the heme iron of NO-Hb, NO would be displaced together with the heme iron. However, the $N_{pyrr}$···NO repulsive interaction increases exponentially as NO approaches the porphyrin plane and finally is in balance with the withdrawing force of His-F8. This is the case of the $\beta^{NO}$ subunit of NO-Hb in the T structure. If the withdrawing force were stronger, either the Fe–$N_\epsilon$(His-F8) bond or Fe–NO bond, presumably the former due to the weaker bond strength, would be broken in the shortest limit of the $N_{pyrr}$···NO distance. Thus cleavage of the Fe–$N_\epsilon$(His-F8) bond takes place. This is the case of the $\alpha^{NO}$ subunit of NO-Hb in the T structure.

In the case of deoxy-Hb, the restraining force against the displacement of the heme iron is the Fe–$N_{pyrr}$ coordination bonds. This would not be very sensitive to the displacement of the heme iron perpendicular to the porphyrin plane. Therefore, the cleavage of the Fe–$N_\epsilon$ bond need not occur even though His-F8 withdraws the heme iron significantly. As a result, the Fe–$N_\epsilon$(His-F8) bond is simply stretched without cleavage in the T structure of deoxy-Hb and the stretch is larger in the $\alpha$ subunit than in the $\beta$ subunit.

Recently Phillips (1978) revealed from the low-temperature X-ray crystallographic analysis that the heme iron of oxy-Mb is displaced toward His-F8 by 0.33 Å with the Fe–$O_2$ bond length of 1.9 Å. Due to the longer Fe–$O_2$ bond length compared with the Fe–NO bond length, the repulsive interaction between $N_{pyrr}$ and $O_2$ is not serious, permitting the displacement of the heme iron toward the proximal histidine side. Presumably the situation would be the same in oxy-Hb, and cleavage of the Fe–$N_\epsilon$(His-F8) bond would not take place for oxy-Hb even when the His-F8 withdraws the heme iron toward itself.

The other factor controlling the stereochemistry of NO–heme within NO-Hb is the thermodynamic stability of the penta- and hexacoordinated NO–heme complexes. Rougee & Brault (1975) studied the binding of various bases and carbon monoxide to ferrous iron porphyrin (eq 1). The values

$$\text{heme–CO} + \text{B} \rightleftharpoons \text{B–heme–CO} \qquad (1)$$

of the binding constant ($K_B^{CO}$) obtained for B = Im and B = 2-MeIm are $4.3 \times 10^7$ $M^{-1}$ and $6 \times 10^5$ $M^{-1}$, respectively. On the other hand, the binding constant of Im to NO–heme complexes ($K_B^{NO}$) was estimated to be ~0.5 $M^{-1}$ by Scholler et al. (1979). $K_B^{NO}$ is much smaller than $K_B^{CO}$. This indicates that the equilibrium for the NO–heme system is significantly shifted to the pentacoordinated structure compared with that for the CO–heme system. In other words, as an intrinsic property of NO–heme complexes, the pentacoordinated structure is thermodynamically more stable than the hexacoordinated one. This was also pointed out by Scheidt et al. (1977) from the fact that the trans ligand of NO in the hexacoordinated NO–heme complex is easily lost even in the crystal.

In conclusion, when the quaternary structure of Hb is switched to the T, His-F8 withdraws the heme iron toward His-F8 more in the $\alpha$ subunit than in the $\beta$ subunit of NO-Hb. The thermodynamic property of the NO–heme complexes and the dynamical action characteristic of the T-structure Hb dually caused cleavage of the Fe–$N_\epsilon$(His-F8) bond in the $\alpha$ subunit of NO-Hb but not in the $\beta$ subunit.

## Acknowledgments

The authors thank Drs. K. Imaizumi and K. Imai for the help in measurements of the oxygen equilibrium curve. K.N. and T.K. thank Professors T. Yamano and Y. Enoki for their continuous interest and encouragement.

## References

Abe, M., Kitagawa, T., & Kyogoku, Y. (1978) *J. Chem. Phys. 69*, 4526–4534.

Cassoly, R. (1974) *C. R. Hebd. Seances Acad. Sci., Ser. D 278*, 1417–1420.

Felton, R. H., & Yu, N.-T. (1978) in *The Porphyrins* (Dolphin, D., Ed.) Vol. 3, Chapter 8, Academic Press, New York.

Fuhrhop, J.-H., & Smith, K. N. (1975) in *Porphyrins and Metalloporphyrins* (Smith, K. M., Ed.) Chapter 19, Elsevier, Amsterdam.

Hendra, P. J., & Loader, E. J. (1961) *Chem. Ind. (London)*, 718–719.

Hori, H., & Kitagawa, T. (1980) *J. Am. Chem. Soc. 102*, 3608–3613.

Imai, K., Morimoto, H., Kotani, M., Watari, H., Hirata, W., & Kuroda, M. (1970) *Biochim. Biophys. Acta 200*, 189–196.

Kenner, G. W., Smith, K. M., & Sutton, M. J. (1978) *Tetrahedron Lett.*, 1303–1306.

Kilmartin, J. V., & Rossi-Bernardi, L. (1970) *Biochem. J. 124*, 31–45.

Kilmartin, J. V., Hewitt, J. A., & Wooton, J. F (1975) *J. Mol. Biol. 93*, 203–218.

Kitagawa, T., Kyogoku, Y., Iizuka, T., & Saito, I. M. (1976) *J. Am. Chem. Soc. 98*, 5169–5173.

Kitagawa, T., Ozaki, Y., & Kyogoku, Y. (1978a) *Adv. Biophys. 11*, 153–192.
Kitagawa, T., Abe, M., & Ogoshi, H. (1978b) *J. Chem. Phys. 69*, 4516–4525.
Kitagawa, T., Nagai, K., & Tsubaki, M. (1979) *FEBS Lett. 104*, 376–378.
Maxwell, J. C., & Caughey, W. S. (1976) *Biochemistry 15*, 388–396.
Monod, J., Wyman, J., & Changeux, J.-P. (1965) *J. Mol. Biol. 12*, 88–118.
Nagai, K., & Kitagawa, T. (1980) *Proc. Natl. Acad. Sci. U.S.A. 77*, 2033–2037.
Nagai, K., Hori, H., Yoshida, S., Sakamoto, H., & Morimoto, H. (1978) *Biochim. Biophys. Acta 532*, 17–28.
Nagai, K., Hori, H., Morimoto, H., Hayashi, A., & Taketa, F. (1979) *Biochemistry 18*, 1304–1308.
Nagai, K., Kitagawa, T., & Morimoto, H. (1980) *J. Mol. Biol. 136*, 271–289.
Nozaki, Y., & Tanford, C. (1967) *Methods Enzymol. 11*, 715–734.
Perutz, M. F. (1970) *Nature (London) 228*, 726–734.
Perutz, M. F., Kilmartin, J. V., Nagai, K., Szabo, A., & Simon, S. R. (1976) *Biochemistry 15*, 378–387.
Phillips, S. E. V. (1978) *Nature (London) 273*, 247–248.
Rein, H., Ristau, O., & Scheler, W. (1972) *FEBS Lett. 24*, 24–26.
Rougee, M., & Brault, D. (1975) *Biochemistry 14*, 4100–4106.
Salhany, J. M., Ogawa, S., & Shulman, R. G. (1974) *Proc. Natl. Acad. Sci. U.S.A. 71*, 3359–3362.
Salhany, J. M., Ogawa, S., & Shulman, R. G. (1975) *Biochemistry 14*, 2180–2190.
Scheidt, W. R., & Frisse, M. E. (1975) *J. Am. Chem. Soc. 97*, 17–21.
Scheidt, W. R., & Piciulo, P. L. (1976) *J. Am. Chem. Soc. 98*, 1913–1919.
Scheidt, W. R., Brinegar, A. C., Ferro, E. B., & Kirner, J. F. (1977) *J. Am. Chem. Soc. 99*, 7315–7321.
Scholler, D. M., Wang, M.-Y. R., & Hoffman, B. M. (1979) *J. Biol. Chem. 254*, 4072–4078.
Shelnutt, J. A., Rousseau, D. L., Friedman, J. M., & Simon, S. R. (1979) *Proc. Natl. Acad. Sci. U.S.A. 76*, 4409–4413.
Shiga, T., Hwang, K.-J., & Tyuma, I. (1969) *Biochemistry 8*, 378–383.
Spaulding, L. D., Chang, C. C., Yu, N.-T., & Felton, R. H. (1975) *J. Am. Chem. Soc. 97*, 2517–2524.
Spiro, T. G. (1975) *Biochim. Biophys. Acta 416*, 169–187.
Spiro, T. G., & Strekas, T. C. (1974) *J. Am. Chem. Soc. 96*, 338–345.
Spiro, T. G., Strong, J. D., & Stein, P. (1979) *J. Am. Chem. Soc. 101*, 2648–2655.
Szabo, A., & Barron, L. D. (1975) *J. Am. Chem. Soc. 97*, 660–662.
Szabo, A., & Perutz, M. F. (1976) *Biochemistry 15*, 4427–4428.
Teraoka, J., & Kitagawa, T. (1980) *J. Biol. Chem.* (in press).
Yonetani, T., & Asakura, T. (1968) *J. Biol. Chem. 243*, 4715–4721.

# Apurinic/Apyrimidinic Endonuclease Sensitive Sites as Intermediates in the in Vitro Degradation of Deoxyribonucleic Acid by Neocarzinostatin†

Kallol K. Bose, Kouichi Tatsumi,‡ and Bernard S. Strauss*

ABSTRACT: Neocarzinostatin (NCS) induces alkali-labile sites in DNA which are stabilized by $NaBH_4$ reduction. The stabilized sites are sensitive to an AP endonuclease from human lymphoma cells. NCS-induced degradation of supercoiled Col E1 DNA proceeds in stepwise fashion with apurinic/apyrimidinic (AP) sites as intermediates. Degradation is increased when reaction occurs in the presence of AP endonuclease, and DNA reacted with NCS can be shown to have numerous AP endonuclease sensitive sites.

The antitumor antibiotic neocarzinostatin (NCS) is a small acidic protein of defined sequence with a molecular weight of 10 700 (Ishida et al., 1965; Meienhofer et al., 1972). NCS cytotoxicity and antitumor activity are thought to be due to its interaction with, and subsequent degradation of, cellular DNA (Ono et al., 1966; Beerman & Goldberg, 1974; Sawada et al., 1974) resulting from reaction at the sites of dT and dA residues in DNA with dT being the preferred substrate (Hatayama et al., 1978; D'Andrea & Haseltine, 1978). Sulfhydryl agents are required for NCS activity (Beerman & Goldberg, 1974), and free thymine and to a lesser extent adenine are released in an amount correlated with the number of strand scissions (Poon et al., 1977; Ishida & Takahashi, 1976). It has been suggested that NCS first produces single-strand breaks in a double-stranded DNA and that the double-strand breaks result from two independent single strand break events (D'Andrea & Haseltine, 1978). These authors suggested that the strand breaks might be produced by a two-stage reaction involving base removal, followed by cleavage of phosphodiester bonds. We were interested in this possible mechanism because of the previous studies from this laboratory on the pathway of degradation of alkylated DNA via apurinic sites. In this communication we show that apurinic/apyri-

† From the Department of Microbiology, The University of Chicago, Chicago, Illinois 60637. *Received August 15, 1979; revised manuscript received June 2, 1980.* This work was supported by grants from the National Institutes of Health (GM 07816, CA 14599, and CP 85669) and the Department of Energy (EY 765-02-2040).

‡ Fellow of the Leukemia Society of America. Present address: Department of Internal Medicine, Division of Hematology and Immunology, Kanazawa Medical University, Uchinada-machi, Kahoku-gun, Ishikawa 920-02, Japan.

0006-2960/80/0419-4761$01.00/0 